SONGSHAN LAKE
MATERIALS LABORATORY

PAPER • OPEN ACCESS

Inheritance factor on the physical properties in metallic glasses

View the article online for updates and enhancements.

Inheritance factor on the physical properties in metallic glasses

Weiming Yang[1,10]**, Jiawei Li**[2,10]**, Hongyang Li**[1]**, Haishun Liu**[3,*] ⓘ**, Jinyong Mo**[3]**, Si Lan**[4,5]**, Maozhi Li**[6]**, Xun-Li Wang**[5,7]**, Jürgen Eckert**[8,9] **and Juntao Huo**[2,*]

[1] School of Mechanics and Civil Engineering, State Key Laboratory for Geomechanics and Deep Underground Engineering, China University of Mining and Technology, Xuzhou 221116, People's Republic of China

[2] CAS Key Laboratory of Magnetic Materials and Devices, Zhejiang Province Key Laboratory of Magnetic Materials and Application Technology, Ningbo Institute of Materials Technology and Engineering, Chinese Academy of Sciences, Ningbo, Zhejiang 315201, People's Republic of China

[3] School of Materials and Physics, China University of Mining and Technology, Xuzhou 221116, People's Republic of China

[4] Herbert Gleiter Institute of Nanoscience, Nanjing University of Science and Technology, 200 Xiaolingwei Avenue, Nanjing 210094, People's Republic of China

[5] Department of Physics, City University of Hong Kong, 83 Tat Chee Avenue, Hong Kong, People's Republic of China

[6] Department of Physics, Beijing Key Laboratory of Opto-electronic Functional Materials and Micro-nano Devices, Renmin University of China, Beijing 100872, People's Republic of China

[7] Center for Neutron Scattering, City University of Hong Kong Shenzhen Research Institute, 8 Yuexing 1st Road, Shenzhen Hi-Tech Industrial Park, Shenzhen 518057, People's Republic of China

[8] Erich Schmid Institute of Materials Science, Austrian Academy of Science, 8700 Leoben, Austria

[9] Department of Materials Science, Chair of Materials Physics, Montanuniversität Leoben, 8700 Leoben, Austria

E-mail: liuhaishun@cumt.edu.cn and huojuntao@nimte.ac.cn

CrossMark

Abstract

Material genetic engineering can significantly accelerate the development of new materials. As an important topic in material science and condensed matter physics, the development of metallic glasses (MGs) with specific properties has largely been the result of trial and error since their discovery in 1960. Yet, property design based on the physical parameters of constituent elements of MGs remains a huge challenge owing to the lack of an understanding of the property inheritance from constitute elements to the resultant alloys. In this work, we report the inherent relationships of the yield strength σ_y, Young's modulus E, and shear Modulus G with the valence electron density. More importantly, we reveal that the electronic density of states (EDOSs) at the Fermi surface (E_F) is an inheritance factor for the physical properties of MGs. The physical properties of MGs are inherited from the specific element with the largest coefficient of electronic specific heat (γ_i), which dominates the value of the EDOS at E_F. This work not only contributes to the understanding of property inheritances but also guides the design of novel MGs with specific properties based on material genetic engineering.

---

[10] These authors made equal contributions.
[*] Authors to whom any correspondence should be addressed.

1. Introduction

As one of the important systems in condensed matter physics and material science, metallic glasses (MGs) have attracted intense attention over the past decades owing to their distinctive properties, e.g. high strength, good corrosion resistance, and excellent soft magnetic properties [1]. Since their discovery in 1960 [2], thousands of MG compositions have been developed based on a wide range of elements [3]. In parallel with experimental research, many theoretical works have sought to establish the relationships between the structure and physical properties of MGs [4–8]. However, theoretical predictions of properties remain challenging due to their disordered structures and metastable states. Consequently, the design of alloys with specific properties has largely been the result of trial-and-error efforts [9]. Material genetic engineering can greatly improve and accelerate the efficiency of the development of new materials [10, 11]. Therefore, revealing the key inheritance factor(s) that determine the properties of MGs is an urgent need for directing the development of new MGs.

Recently, Ma and Wang *et al* [12–14] demonstrated that a variety of MGs inherit their elastic modulus from the base components. Furthermore, in subsequent studies, other physical properties of MGs have been revealed to be related to the corresponding properties of the principal elements. Examples of this phenomenon include Gd-, Ho-, Dy-, Er-, and La-based MGs with promising magnetocaloric properties [15–17], Nd-, Pr-, and Sm-based MGs showing hard magnetic behavior [18], Ce-based MGs that display heavy fermionic behavior [19]; and superconductive MG systems exploiting the superconductive properties of La, Fe, Zr, Hf, and Cu [20–23]. While, for other MGs [24], it is not always the case. Many Cu-based MGs show elastic moduli that are markedly different from those of their base components (see table S1). For example, the bulk modulus of the $Cu_{60}Zr_{20}Hf_{10}Ti_{10}$ glass is quite different from that of its base element Cu and is closer to the bulk modulus of Zr [13]. This underlines that the key inheritance factors determining MG properties are still unclear. The above results raise the following questions: what is the key factor that determines property inheritance in MGs? Revealing the physical parameters of the components that determine these properties is highly important for understanding the inheritance phenomenon and for accelerating the design of MGs with tailored properties.

In this work, we reveal the inheritance factor of physical properties from the perspective of electronic structure by analyzing a total of 90 MG compositions. We have found a universal scaling law that can be rationalized with the fundamental thermodynamics' principles [25, 26] and Fermi sphere-Brillouin zone interactions [27, 28]. Based on this scaling law, we provide a close correlation between the mechanical properties and a certain component that dominates the electronic density of states (EDOSs) at the Fermi surface (E_F) in MGs. These findings guide the design of novel MGs with desirable properties during material genetic engineering.

2. Materials and methods

$Cu_{64}Zr_{36}$ and $Ni_{45}Ti_{20}Zr_{25}Al_{10}$ (at. %) MGs with nominal compositions were prepared by arc-melting of a mixture of pure Cu (99.99%), Zr (99.99%), Ni (99.99%), Ti (99.99%) and Al (99.99%) in a highly purified argon atmosphere. Glassy ribbons were produced from these master alloys by rapid quenching onto a single copper wheel at a speed of 45 m s^{-1}. $Fe_{80}P_{13}C_7$ and $Fe_{74}Mo_6P_{13}C_7$ (at. %) MGs were prepared by torch-melting a mixture of pure Fe (99.9 mass %), Mo (99.9 mass %), C (99.95 mass %), and Fe_3P (99.5 mass %) in a clear fused-silica tube under a high-purity argon atmosphere by a torch. The as-prepared master alloy ingots were fluxed in a fluxing agent composed of B_2O_3 and CaO with a mass ratio of 3:1 at an elevated temperature for 4 h under a vacuum with a pressure of ∼10 Pa. After fluxing, each ingot was re-melted and cast into a copper mold with an inner diameter of 1.0 mm under a high-purity argon atmosphere.

The glassy nature of the obtained samples was ascertained by x-ray diffraction (D8 Advance, Bruker, Germany) using Cu K_α radiation and by differential scanning calorimetry (DSC-404, NETZSCH, Germany) with a heating rate of 0.67 K s^{-1}. The bonding states were evaluated by x-ray photoelectron spectroscopy (XPS) using a Kratos AXIS ULTRA^{DLD} instrument with a monochromic Al K_α x-ray source ($h\nu$ = 1486.6 eV). The power was 120 W and the x-ray spot size was set to 700 × 300 μm. The pass energy of the XPS analyzer was set at 20 eV. The base pressure of the analysis chamber was greater than 5 × 10^{-9} Torr. All of the spectra were calibrated using the binding energy of C 1 *s* (284.8 eV) as the reference, and the etching conditions of beam energy of 2 kV, extractor current of 100 μA, and raster size of 4 mm. Oxygen-free surfaces of glassy samples were obtained by Ar-ion sputtering. Young's modulus and shear modulus were determined using a Quasar RUSpec resonant ultrasound spectrometer. The low-temperature specific heats of the studied amorphous alloys were evaluated using a physical property measurement system (Model-9, Quantum Design Systems, USA). The specific heat measurements were performed in triplicate and the final data were obtained by averaging the three results. The relative error for the specific heat measurements is less than 2%.

Molecular dynamics calculations were performed using the Vienna *ab initio* simulation package [29]. All simulations were carried out in the canonical ensemble with the temperature controlled by the Nose thermostat [30]. Cubic supercells

containing 100 atoms were used, and the dimensions of the cells were estimated according to the alloy densities at room temperature. The cells were first melted and equilibrated at 2000 K, and then gradually cooled first to 1000 K and then to 300 K at a cooling rate of 1.67×10^{14} K s^{-1} with a time step of 3 fs. A $5 \times 5 \times 5$ Monkhorst-Pack mesh was used for k-point sampling, and the EDOSs were calculated considering spin polarization.

3. Results and discussion

Figures 1(a)–(d) show the comparisons of Young's moduli (E) and shear moduli (G) between the $Cu_{64}Zr_{36}$, $Ni_{45}Ti_{20}Zr_{25}Al_{10}$, $Fe_{80}P_{13}C_7$ and $Fe_{74}Mo_6P_{13}C_7$ glassy samples (the glassy nature of samples was shown in figure S1) and their components, respectively. In figures 1(a) and (b), the values of elastic moduli are close to those of a single element, but this element is not the major component. For instance, for the $Ni_{45}Ti_{20}Zr_{25}Al_{10}$ glass, E is 114 GPa, which is quite close to that of pure polycrystalline Ti (116 GPa) but is different from that of Ni (200 GPa) and Zr (98 GPa). This is unusual because the minor component rather than the major component appears to be responsible for the properties of MGs. An examination of figures 1(c) and (d) show that the elastic moduli are close to the corresponding values of their major component Fe, but minor changes in the Mo component (e.g. through microalloying) affect the values of the elastic moduli. E of $Fe_{80}P_{13}C_7$ glass can be dramatically enhanced from 137 to 174 GPa, and G increases from 49 to 65 GPa when 6 at. % Mo was added. This phenomenon seems contradictory but is curious. It is well known that the interatomic bonding controls the elastic moduli of MGs [31] and the characteristics of interatomic bonds are mostly determined by the valence electrons (*d, p,* and/or *s*) [32]. To reveal the mechanism of inheritance in MGs, the XPS valence-band spectra, and spin-polarized total and partial DOS of the valence electrons in the corresponding MGs were obtained as shown in figures 1(a^1)∼(d^1), respectively. The EDOS at E_F of $Cu_{64}Zr_{36}$ and $Ni_{45}Ti_{20}Zr_{25}Al_{10}$ MGs are dominated by the d electrons of Zr and Ti, respectively, as shown in figures 1(a^1) and (b^1), in good agreement with previous results [33]. As shown in figures 1(c^1) and (d^1), Fe contributes to most of the EDOS in the Fe-based MGs at E_F, while the Mo d electrons also make a significant contribution to the

EDOS at E_F in $Fe_{74}Mo_6P_{13}C_7$ (figure S2). It is observed that the modulus inheritance and electronic structure are correlated, namely, the elastic moduli of MGs are mainly inherited from the elements that dominate the EDOS at the E_F in MGs.

To further explore the underlying physics of inheritance, the relationship between the elastic modulus and structural parameters was investigated. In previous studies, the elastic modulus of MGs was found to have a clear relationship to the glass transition temperature T_g and molar volume V [7, 34]. The inherent relationship of E with T_g and V of MGs in a universal scaling equation is given by [25, 26]:

$$E = 3R\left(\frac{2}{\varepsilon_E}\right)\frac{T_g - T_0}{V} \quad (1)$$

where R is the gas constant, T_0 is room temperature, ε_E is the room temperature elastic limit of bulk MGs (BMGs) that is approximately 2% [35]. Since $E = \sigma_y/\varepsilon_E$ and $E = 2.61\,G$ [24], we can thus obtain a universal scaling relationship between σ_y, G, and $(T_g–T_0)/V$.

Recently, fractal concepts have been introduced to describe atomic structure [36, 37]. These models have been invoked to explain the widely observed noncubic power laws (D) correlating the positions of the first sharp diffraction peak, q_1, with V [37], that is:

$$V \sim (1/q_1)^D. \quad (2)$$

From equations (1) and (2), a strong dependence of the mechanical properties on the structural vector q_1 can be obtained as follows:

$$E = \frac{6R(T_g - T_0)q_1^D}{C_1\varepsilon_E} \quad (3)$$

where C_1 is a constant. The above relationship is generally applicable to different types of MGs, independent of their chemical compositions and bonding types. Thus, different types of MGs should follow a similar underlying mechanism of deformation and fracture. Generally, an increase in T_g and q_1 will result in a stronger MG and vice versa. In figure 2, we plotted the correlations between the mechanical properties σ_y (a), E (b), and G (c) and q_1 for 57 MGs (the data are summarized in table S2) as solid lines. It is observed that equation (3) fits the experimental results well, verifying the existence of an intrinsic correlation. The value of the exponent D extracted from the fitting (2.45) is consistent with $D = 2.3$ [37] and 2.5 [38] that have been measured for MGs in previous work. This indicates that although the fractal atomic packing in MGs has not been proven [39], the conclusions obtained by using this fractal model are acceptable and are in good agreement with the experimental results.

Furthermore, many studies [27, 28, 41] have shown that MGs are stabilized when the assumed spherical Fermi surface coincides with the diffused pseudo-Brillouin zone boundary, which can be expressed as $q_1 = 2k_F$, where k_F is the Fermi wave vector. This is also known as Fermi surface-Brillouin zone interaction or the Hume-Rothery stabilization mechanism [42]. All binary and some ternary MGs compositions have
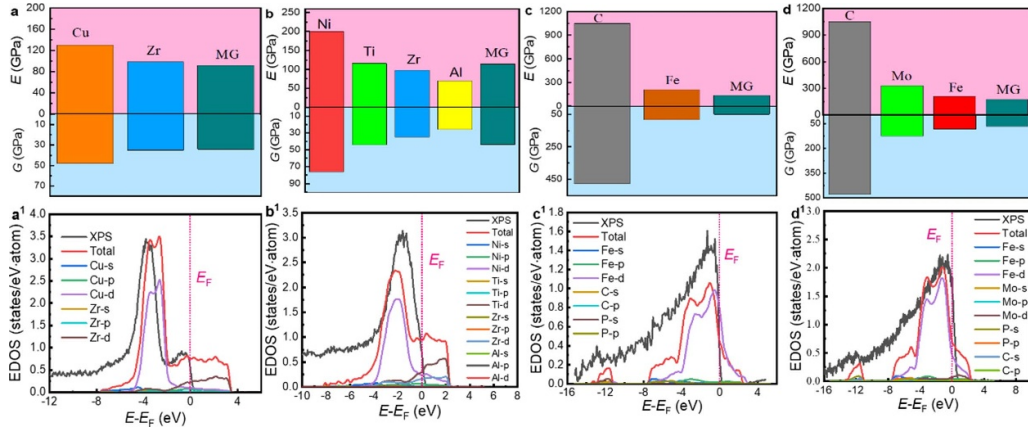
Figure 1. Comparisons of Young's moduli (E) and shear moduli (G) for the (a) $Cu_{64}Zr_{36}$, (b) $Ni_{45}Ti_{20}Zr_{25}Al_{10}$, (c) $Fe_{80}P_{13}C_7$ and (d) $Fe_{74}Mo_6P_{13}C_7$ glassy samples and their components. (a1)$\sim$(d1) XPS spectra and electronic densities of states for the $Cu_{64}Zr_{36}$, $Ni_{45}Ti_{20}Zr_{25}Al_{10}$, $Fe_{80}P_{13}C_7$, and $Fe_{74}Mo_6P_{13}C_7$ glassy samples, respectively.
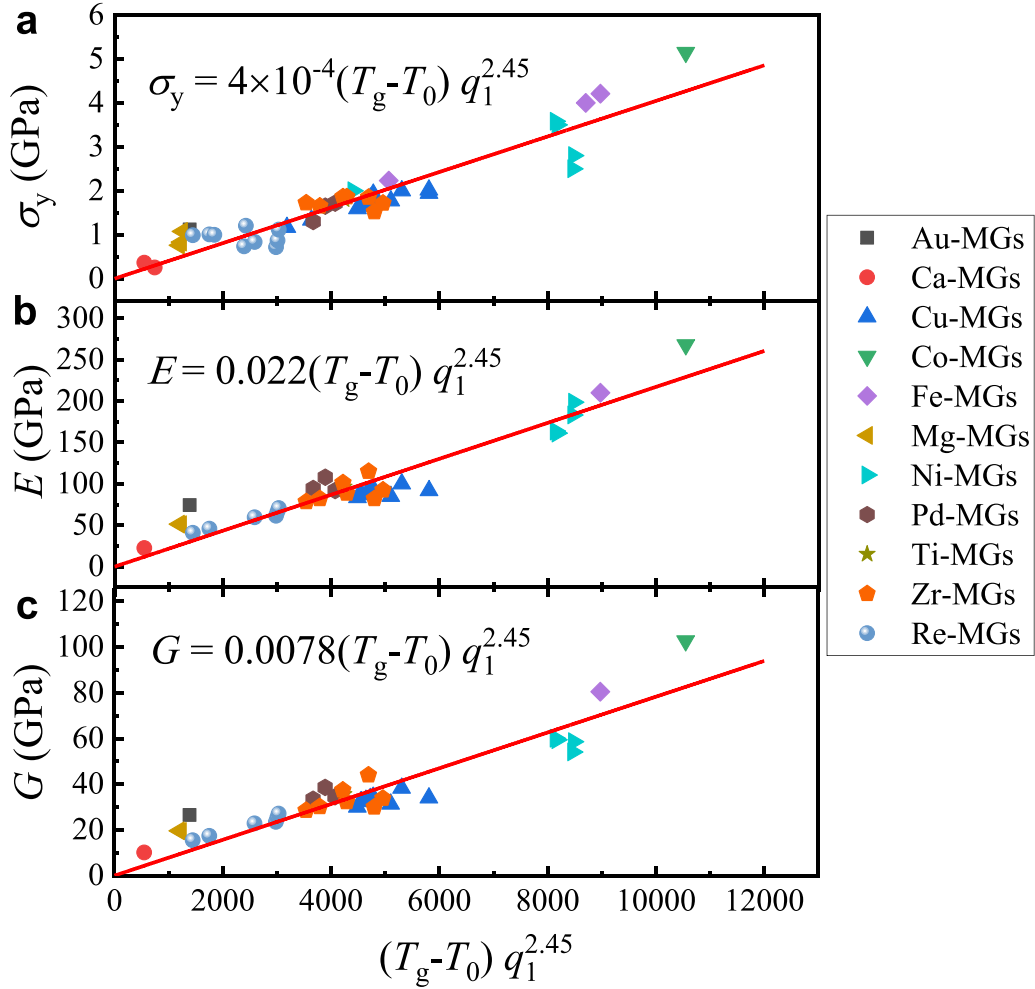
Figure 2. Relationship between yield strength σ_y (a), Young's modulus E (b), shear modulus G (c), T_g, and structural vector q_1 for 57 MGs [40].

been precisely verified experimentally to satisfy the stability criterion [43]. Then, a universal correlation between E and k_F can be obtained as:

$$E = \frac{2^D \cdot 6R(T_g - T_0)k_F^D}{C_1 \varepsilon_E}. \qquad (4)$$

On the one hand, k_F can be given by $k_F = 2\pi \left(\frac{3\rho}{8\pi}\right)^{1/3}$ [28], where ρ is the valence electron density. The correlation between E and ρ can then be described by:
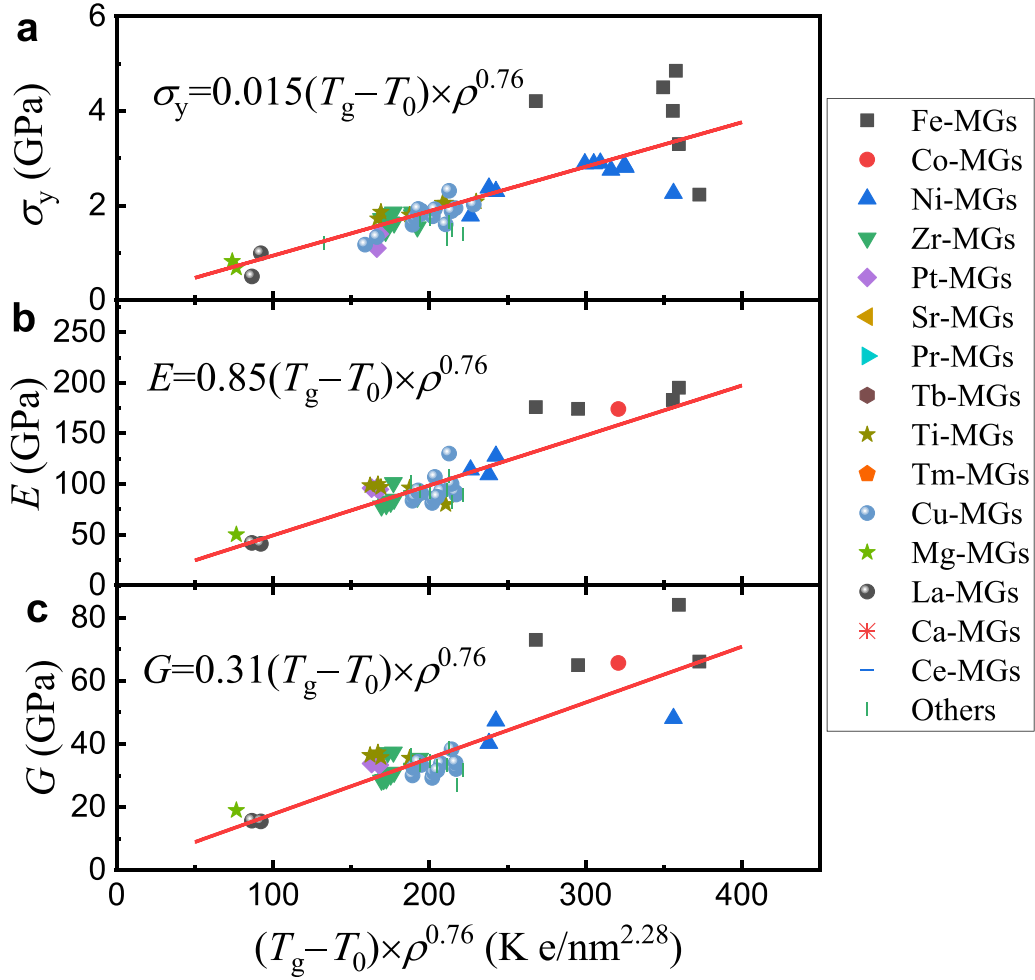
$$E = C(T_g - T_0)\rho^{D/3} \qquad (5)$$

Figure 3. Relationship between yield strength σ_y (a), Young's modulus E (b), shear modulus G (c), glass transition temperature T_g, and valence electron density ρ for a variety of MGs [14, 24, 40].

where C is a constant. It is noted that equation (5) is based on the assumption that q_1 represents the effect of both atomic spacing V and valence electron density ρ. Fortunately, MGs can be considered metallic materials with isotropic electron clouds. Despite the lack of long-range periodicity in their atomic structures, MGs can be considered virtually isotropic (i.e. a close-to-spherical symmetry) even down to the atomic level [40]. Thus, the $2k_F = q_1$ relationship is valid, as can be further confirmed in figure 3. As shown in figure 3(a), equation (5) fits the experimental data well (the data are also summarized in table S3), demonstrating that σ_y of MGs is intrinsically linked with ρ, which is also consistent with previous works [44]. A remarkable agreement was also observed between the calculated and measured E and G values of various MGs, as shown in figures 3(b) and (c), respectively. Thus, equation (5) demonstrates that in MGs, Young's modulus is directly related to the valence electron density.

On the other hand, EDOS at the Fermi level $n(E_F)$ and k_F is also related to each other by $k_F = \frac{n(E_F)}{\pi^2\hbar^2 mV}$ [45]. Then, the relationship between E and $n(E_F)$ can be expressed as:

$$E = C(T_g - T_0)\left[\frac{n(E_F)}{V}\right]^D. \tag{6}$$

Equation (6) indicates that the mechanical properties of MGs depended on the EDOS at E_F. A straightforward way to obtain experimental information regarding the EDOS at E_F is to measure the low-temperature specific heat C_p. The EDOS at E_F is directly related to the linear term temperature coefficient of the electronic specific heat [46], $\gamma = (1/3)\pi^2 k_B^2(1 + \lambda_{ep})$ $n(E_F)$, where k_B is the Boltzmann constant and λ_{ep} accounts for the enhancement of γ due to the electron-phonon interaction. Since the electron-phonon enhancement turns out to be of minor importance [47], the composition dependence of γ already reflects the band structure at E_F well. The relationship between E and γ can be approximately expressed as:

$$E = A(T_g - T_0)\left[\frac{\gamma}{V}\right]^D + B \tag{7}$$

where A and B are constants. This indicates that the mechanical properties should be related to γ and $n(E_F)$ values of MGs. To confirm this correlation, the C_p values of $Cu_{64}Zr_{36}$, $Ni_{45}Ti_{20}Zr_{25}Al_{10}$, $Fe_{80}P_{13}C_7$, and $Fe_{74}Mo_6P_{13}C_7$ BMGs are presented in figure 4(a). C_p can be separated into the linear electronic contribution (γT) and the cubic Debye's contribution (δT^3) below 20 K [48], $\delta = 12\pi^4 R/(5\theta_D^3)$, where θ_D is the Debye temperature. The relationship between C_p and T can be
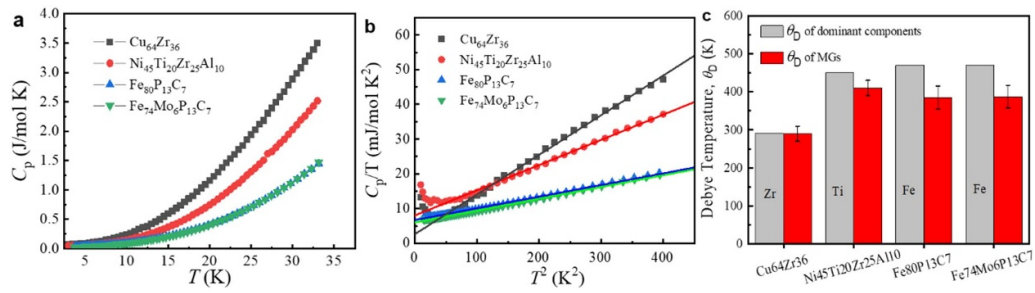
Figure 4. Specific heat C_p of the MGs in the temperature range from 3 to 33 K. (a) Specific heat plotted versus the temperature. (b) Specific heat, shown as C_p/T vs T^2, where the solid lines are the results of the fitting of the specific heat data to $C_p/T = \gamma + \delta T^2$. (c) Histograms of θ_D for MGs and one of their dominant components.

Table 1. Summary of the glass transition temperature T_g, calculated molar volume V, yield strength σ_y, Young's modulus E, shear modulus G, and linear term low-temperature coefficient of the electronic specific heat γ of 15 MGs [14, 24]. The values of molar volumes V of the MGs are calculated according to the rule of mixtures [49].

Label	Composition	T_g (K)	V (cm^3 mol^{-1})	σ_y (GPa)	E (GPa)	G (GPa)	γ (mJ mol^{-1} K^2)	References.
A	Cu$_{64}$Zr$_{36}$	744	9.646	1.94	92	34	2.64	This work
B	Ni$_{45}$Ti$_{20}$Zr$_{25}$Al$_{10}$	733	9.110	2.37	114	44	8.01	This work
C	Fe$_{74}$Mo$_6$P$_{13}$C$_7$	715	6.999	3.30	173	65	6.00	This work
D	Fe$_{80}$P$_{13}$C$_7$	669	6.740	3.14	137	49	6.70	This work
E	Cu$_{50}$Zr$_{50}$	733	10.451	1.92	85	32	4.30	[50]
F	(Fe$_{0.8}$Co$_{0.2}$)$_{72}$B$_{20}$Si$_4$Nb$_4$	830	6.218	4.17	205	78	6.94	[51]
G	Zr$_{46.75}$Ti$_{8.25}$Cu$_{7.5}$Ni$_{10}$Be$_{27.5}$	623	9.930	1.83	100	37.2	2.82	[52]
H	Zr$_{41}$Ti$_{14}$Cu$_{12.5}$Ni$_{10}$Be$_{22.5}$	620	9.788	1.8	101	37.4	3.03	[53]
I	Co$_{56}$Ta$_9$B$_{35}$	945	5.923	5.80	240	91.5	7.10	[54]
J	Pd$_{40}$Ni$_{10}$Cu$_{30}$P$_{20}$	564	7.959	1.52	98	35.1	0.67	[52]
K	Cu$_{60}$Zr$_{20}$Hf$_{10}$Ti$_{10}$	734	9.501	1.95	101	36.9	2.73	[55]
L	Pd$_{77.5}$Cu$_6$Si$_{16.5}$	630	8.742	1.55	96	34.8	0.40	[56]
M	Cu$_{45}$Zr$_{45}$Al$_7$Gd$_3$	670	10.645	1.81	90.6	32.9	4.90	[57]
N	Pd$_{40}$Ni$_{40}$P$_{20}$	630	7.6805	1.84	91.9	32.7	2.19	[50]
O	Zr$_{52.5}$Ti$_5$Cu$_{17.9}$Ni$_{14.6}$Al$_{10}$	672	10.768	1.77	88.6	32.3	3.44	[58]

fitted using $C_p/T = \gamma + \delta T^2$ with different γ and δ. The results of this fit are shown in figure 4(b) and demonstrate the good linear relationships between C_p/T and T^2 for these MGs. The θ_D values of these MGs derived from the δ coefficients and those of their components are compared in figure 4(c). Similar to EDOS and moduli inheritance, the θ_D of these MGs are also inherited from one of their components. The γ values of MGs, together with their σ_y, *E, G, V,* and T_g are summarized in table 1.

The relationships between σ_y, *E*, and *G* vs γ/V are shown by the solid lines plotted in figure 5. It is observed that equation (7) fits the experimental results very well, verifying the existence of a correlation between the mechanical properties and γ values. Generally, two characteristics of the electron-density distribution, namely bond directionality and charge polarizability, determine the strength and modulus [31]. In principle, the bonding characteristics mainly depend on the EDOS at E_F. The γ values are determined by all the electrons contained in the components and their hybridization [59, 60]. If the effects of covalent bonds and electron hybridization are not considered, the γ of a MG shows a correlation with a weighted average of the coefficient of the electronic specific heat γ_i for the constituent element, $\gamma = \Sigma \gamma_i \times f_i$, where

f_i denotes the atomic percentage of the constituent element. It indicates that the component with the largest $\gamma_i \times f_i$ that dominates the EDOS at E_F has a decisive influence on the physical properties of MGs. The minor changes in atom components (e.g. through microalloying) may significantly change the EDOS of an MG and accordingly influence the physical properties. As shown in figure 6, $\gamma_{Cu} = 0.7$ mJ mol^{-1} K^2 is much smaller than $\gamma_{Zr} = 2.8$ mJ mol^{-1} K^2, which means that the EDOS at E_F of Cu–Zr glassy systems is mainly dominated by Zr rather than by Cu. Moreover, $\gamma_{Ce} = 1620$ mJ mol^{-1} K^2 is much larger than $\gamma_{La} = 10$ mJ mol^{-1} K^2. In (Ce$_x$La$_{100-x}$)-based MGs ($x = 10 \sim 80$) [61], even though the Ce content is very low, the EDOS value at E_F of (Ce$_{10}$La$_{90}$)$_{68}$Al$_{10}$Cu$_{20}$Co$_2$ glass is mainly determined by Ce [62]. Correspondingly, the elastic moduli of (Ce$_{10}$La$_{90}$)$_{68}$Al$_{10}$Cu$_{20}$Co$_2$ MG are closer to those of Ce rather than to those of La (the data are also summarized in table S4). These results further confirm that EDOS at E_F or the γ_i value is an inheritance factor of physical properties in MGs, i.e. the basic physical properties of MGs are inherited from a certain component with the largest $\gamma_i \times f_i$. The properties of the MGs can be judged preliminarily through the γ_i values in figure 6 and their atomic percentage f_i.
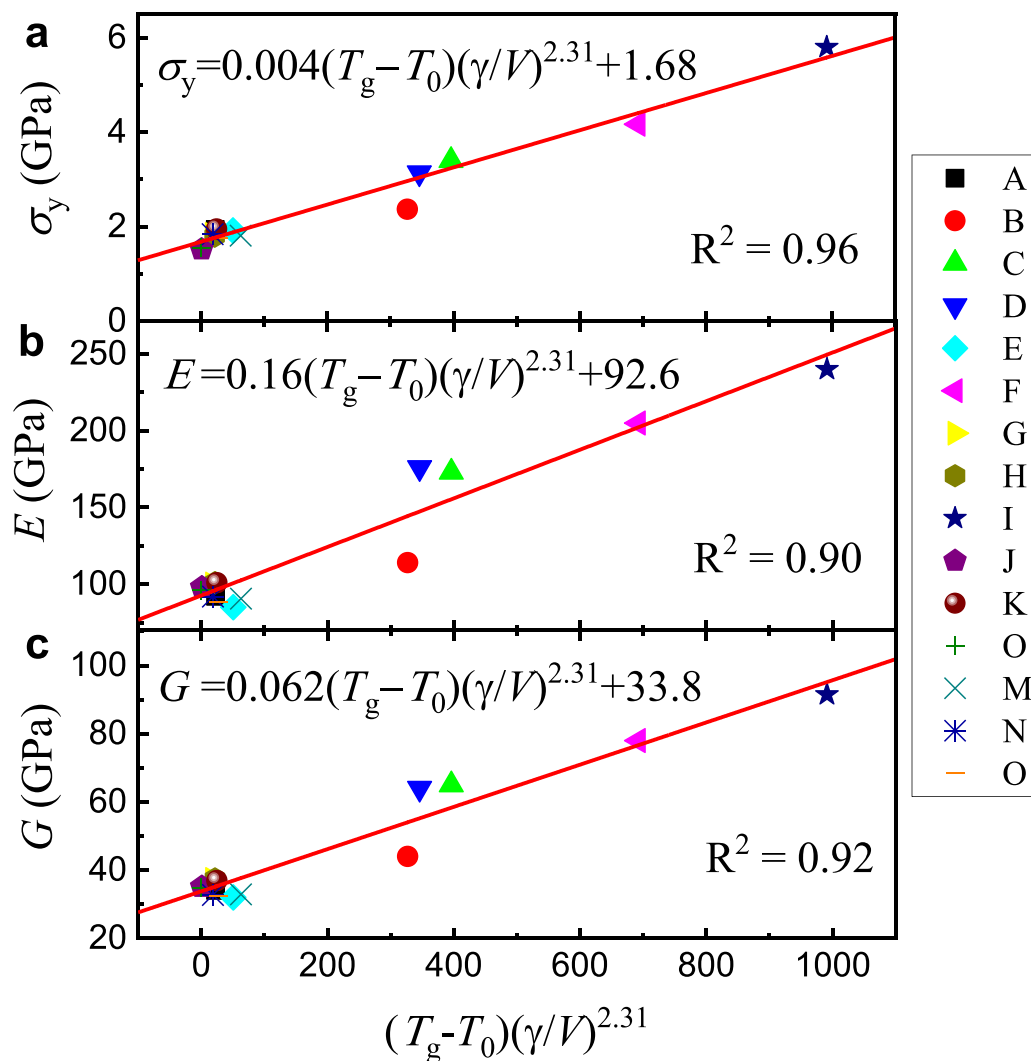
Figure 5. Relationship between yield strength σ_y (a), Young's modulus E (b), shear modulus G (c), glass transition temperature T_g, and low-temperature coefficient of the electronic specific heat γ for 15 MGs.

Figure 6. Experimental values [63] of the linear term temperature coefficients γ_i of electronic specific heat for a great number of elements.

Table 2. The physical properties of some typical metallic glasses inherit from their component.

Physical properties	MGs	Values of MGs	Dominate components	Values of components	References
Magnetocaloric effect	$Gd_{53}Al_{24}Co_{20}Zr_3$	9.40 (5T)	Gd	9.8 (5T)	[16]
	$Gd_{33}Er_{22}Al_{25}Co_{20}$	9.47 (5T)	Gd	9.8 (5T)	[16]
	$Gd_{55}Ni_{25}Al_{20}$	9.76 (5T)	Gd	9.8 (5T)	[64]
Debye temperature	$Zr_{55}Al_{10}Ni_{10}Cu_{15}Be_{10}$	297 K	Zr	291 K	[24]
	$Fe_{60}Cr_{10}Mo_9C_{13}B_6Er_2$	471 K	Fe	470 K	[24]
	$Ca_{65}Mg_{8.54}Li_{9.96}Zn_{16.5}$	221 K	Ca	230 K	[24]
Superconducting temperature	$La_{60}Cu_{20}Ni_{10}Al_{10}$	2.5 K	La	6.0 K	[20]
	$Fe_{30}Zr_{70}$	1.9 K	Fe	2.1 K	[65]
	$Zr_{54}Cu_{46}$	0.9 K	Zr	0.85 K	[66]
	$Zr_{50}Cu_{50}$	0.7 K	Zr	0.85 K	[66]

Although we have mainly focused on the inheritance factor of elastic moduli in MGs, the other physical properties such as magnetocaloric effects, Debye temperature, and superconducting temperature also follow the inheritance, as examples in table 2. The physical properties of the MGs are dominated by the major contribution composition to the γ (the EDOS at E_F). Thus, the γ_i values in figure 6 can be used to design tailored properties of MGs by high-throughput computational simulation and/or machine learning.

It was found that elastic properties of MGs are primarily determined by their base pure polycrystalline components [12], and usually increased by about 30% after crystallization [67]. In principle, trends similar to the physical properties inheritance and correlations observed here should also exist for intermetallic compounds; however, due to a large number of dislocations and/or defects in MGs after crystallization, the factors affecting mechanical properties are more complex, and it is difficult to determine quantitative relationships between EDOS and mechanical properties. Furthermore, due to covalent bonds and *sp-d* hybridization, the assignment of valence electrons is complicated in most alloys containing transition metals, metalloids, and/or rare earth [59, 60]. The data scatter observed for metalloid glasses, such as Fe-, Co-, Ni-, Pd-, and Pt-based MGs, may be considered due to the perturbations stemming from the above-mentioned effects. In particular, Fe-based MGs usually contain non-metallic elements such as B, Si, P, and C [68]. These elements will form covalent bonding with Fe and generate *sp-d* hybridization [59]. This results in that the electron's contribution γ_i to the parameter γ is no longer a weighted average. Therefore, the scattering of Fe-based MGs is far more than that of others. Fortunately, the transition metals can be treated as if they have one free electron per atom [27], and the presence of the Fermi sphere-Brillouin zone interaction has been both theoretically and experimentally confirmed in transition metal and rare earth MGs [28, 69]. The *E, G,* and σ_y are complex material parameters that may be influenced by the 'micro-structure', fracture and deformation mode, preparation, loading conditions, specimen size, and aspect ratio geometry. It is important to mention that the T_g and molar volume V depends on the thermal history, such as aging, rejuvenation, and processing conditions. The structural heterogeneity and atomic density

fluctuation froze during rapid quenching are also expected to result in the fluctuation of free-volume regions, valence electron density, and low-temperature specific heat. In the free-volume regions, where mechanical coupling to the surrounding atomic environment is weak, inelastic relaxation becomes possible by local atom rearrangements, without affecting the surrounding atomic environment significantly [25, 70]. Thus, these sites are the preferred regions to initiate the scattering of data. If these effects can be ruled out, the theoretical and experimental values of MGs will likely show better agreement. Namely, considering the large phase space of possible metallic glass compositions and their multicomponent nature, their exploration as the result of trial-and-error efforts will be very time-consuming. By contrast, if it is known that the EDOS at E_F is controlled by a certain element, then only calculations for the properties of that element are possible to predict the properties of MGs. Thus, this work may help to design novel MGs with specific properties.

4. Conclusions

In summary, we have successfully derived a universal scaling law based on fundamental thermodynamics' principles and Fermi sphere-Brillouin zone interactions. The linearity between mechanical properties and glass transition temperature unambiguously demonstrates that the linear elastic properties of MGs are dominated by structural vector and/or valence electron density. It was found that the EDOS at E_F is an inheritance factor of physical properties in MGs, i.e. the elastic moduli of MGs are inherited from the components of the MGs that dominate the EDOS at E_F. This work can be used to design novel MGs with specific properties and will have a significant impact on material genetic engineering.

Author contributions

W M Yang, J W Li, H S Liu, and J T Huo conceived and designed the research and analysis. H Y Li contributed to data collection. J Y Mo and M Z Li performed the MD simulations. W M Yang, H S Liu, S Lan, X-L Wang, M Z Li, J Eckert, and J T Huo performed the data analysis and wrote the paper with assistance from all authors. All authors contributed to the analysis of the results and the discussion in the manuscript.

Conflict of interest

The authors declare no competing financial interests.

ORCID iD

Haishun Liu ⓘ https://orcid.org/0000-0003-4505-5980

References

[1] Zhang J Y *et al* 2022 Recent development of chemically complex metallic glasses: from accelerated compositional design, additive manufacturing to novel applications *Mater. Futures* **1** 012001

[2] Clement W, Willens R H and Duwez P 1960 Non-crystalline structure in solidified Gold-Silicon alloys *Nature* **187** 869–70

[3] Xiong J, Shi S-Q and Zhang T-Y 2020 A machine-learning approach to predicting and understanding the properties of amorphous metallic alloys *Mater. Des.* **187** 108378

[4] Spaepen F 1977 A microscopic mechanism for steady state inhomogeneous flow in metallic glasses *Acta Metall.* **25** 407–15

[5] Langer J 2006 Shear-transformation-zone theory of deformation in metallic glasses *Scr. Mater.* **54** 375–9

[6] Chen Y, Jiang M Q and Dai L H 2011 How does the initial free volume distribution affect shear band formation in metallic glass? *Sci. China Phys. Mech. Astron.* **54** 1488–94

[7] Zaccone A and Terentjev E M 2013 Disorder-assisted melting and the glass transition in amorphous solids *Phys. Rev. Lett.* **110** 178002

[8] Zaccone A and Scossa-Romano E 2011 Approximate analytical description of the nonaffine response of amorphous solids *Phys. Rev.* B **83** 184205

[9] Li M-X, Zhao S-F, Lu Z, Hirata A, Wen P, Bai H-Y, Chen M, Schroers J, Liu Y and Wang W-H 2019 High-temperature bulk metallic glasses developed by combinatorial methods *Nature* **569** 99

[10] Sparks T D, Kauwe S K, Parry M E, Tehrani A M and Brgoch J 2020 Machine learning for structural materials *Ann. Rev. Mater. Res.* **50** 27

[11] Fan Z, Ding J and Ma E 2020 Machine learning bridges local static structure with multiple properties in metallic glasses *Mater. Today* **40** 48

[12] Ma D, Stoica A D, Wang X L, Lu Z P, Clausen B and Brown D W 2012 Elastic moduli inheritance and the

weakest link in bulk metallic glasses *Phys. Rev. Lett.* **108** 085501

[13] Wang W H 2012 Metallic glasses: family traits *Nat. Mater.* **11** 275–6

[14] Wang W H 2012 Properties inheritance in metallic glasses *J. Appl. Phys.* **111** 123519

[15] Luo Q and Wang W H 2010 Magnetocaloric effect in rare earth-based bulk metallic glasses *J. Alloys Compd.* **495** 209–16

[16] Luo Q, Zhao D, Pan M and Wang W 2006 Magnetocaloric effect in Gd-based bulk metallic glasses *Appl. Phys. Lett.* **89** 081914

[17] Li F, Feng J, Yi J, Wang G, Wang J-Q and Huo J 2020 Magnetocaloric properties of LaFe11.4Si1.6 based amorphous alloys *J. Alloys Compd.* **845** 156191

[18] Wei B, Löser W, Xia L, Roth S, Pan M, Wang W and Eckert J 2002 Anomalous thermal stability of Nd-Fe-Co-Al bulk metallic glass *Acta Mater.* **50** 4357–67

[19] Tang M, Bai H, Wang W, Bogdanov D, Winzer K, Samwer K and Egami T 2007 Heavy-fermion behavior in cerium-based metallic glasses *Phys. Rev.* B **75** 172201

[20] Tang M B, Bai H Y, Pan M X, Zhao D Q and Wang W H 2005 Bulk metallic superconductive $La_{60}Cu_{20}Ni_{10}Al_{10}$ glass *J. Non-Cryst. Solids* **351** 2572–5

[21] Tenhover M and Johnson W 1983 Superconductivity and the electronic structure of Zr-and Hf-based metallic glasses *Phys. Rev.* B **27** 1610

[22] Onn D, Wang L and Fukamichi K 1983 Superconductivity in Fe-Zr, Ni-Zr and Cu-Zr amorphous metal alloys: analysis of low temperature specific heat *Solid State Commun.* **47** 479–83

[23] Vora A M and Gandhi A L 2020 Theoretical investigation of superconducting state parameters of some bulk metallic glasses using pseudopotential approach *J. Supercond. Nov. Magn.* **33** 323–30

[24] Wang W H 2012 The elastic properties, elastic models and elastic perspectives of metallic glasses *Prog. Mater. Sci.* **57** 487–656

[25] Liu Y, Liu C, Wang W, Inoue A, Sakurai T and Chen M 2009 Thermodynamic origins of shear band formation and the universal scaling law of metallic glass strength *Phys. Rev. Lett.* **103** 065504

[26] Yang B, Liu C T and Nieh T 2006 Unified equation for the strength of bulk metallic glasses *Appl. Phys. Lett.* **88** 221911–3

[27] Nagel S and Tauc J 1975 Nearly-free-electron approach to the theory of metallic glass alloys *Phys. Rev. Lett.* **35** 380

[28] Dong C, Wang Z-J, Zhang S and Wang Y-M 2020 Review of structural models for the compositional interpretation of metallic glasses *Int. Mater. Rev.* **65** 286–96

[29] Kresse G and Furthmüller J 1996 Efficiency of *ab-initio* total energy calculations for metals and semiconductors using a plane-wave basis set *Comput. Mater. Sci.* **6** 15–50

[30] Nosé S 1984 A unified formulation of the constant temperature molecular dynamics methods *J. Chem. Phys.* **81** 511–9

[31] Eberhart M E, Latanision R and Johnson K 1985 Overview no. 44: the chemistry of fracture: a basis for analysis *Acta Metall.* **33** 1769–83

[32] Niu H, Chen X-Q, Liu P, Xing W, Cheng X, Li D and Li Y 2012 Extra-electron induced covalent strengthening and generalization of intrinsic ductile-to-brittle criterion *Sci. Rep.* **2** 1–6

[33] Oelhafen P, Hauser E and Güntherodt H-J 1980 Varying *d*-band splitting in glassy transition metal alloys *Solid State Commun.* **35** 1017–9

[34] Egami T 1997 Universal criterion for metallic glass formation *Mater. Sci. Eng.* A **226** 261–7

[35] Cubuk E D, Ivancic R, Schoenholz S S, Strickland D, Basu A, Davidson Z, Fontaine J, Hor J L, Huang Y-R and Jiang Y

2017 Structure-property relationships from universal
signatures of plasticity in disordered solids *Science*
358 1033–7

[36] Chen D Z, Shi C Y, An Q, Zeng Q, Mao W L, Goddard W A
and Greer J R 2015 Fractal atomic-level percolation in
metallic glasses *Science* **349** 1306–10

[37] Ma D, Stoica A D and Wang X-L 2009 Power-law scaling and
fractal nature of medium-range order in metallic glasses
Nat. Mater. **8** 30–34

[38] Zeng Q, Lin Y, Liu Y, Zeng Z, Shi C Y, Zhang B, Lou H,
Sinogeikin S V, Kono Y and Kenney-Benson C 2016
General 2.5 power law of metallic glasses *Proc. Natl Acad.
Sci.* **113** 1714–8

[39] Ding J, Asta M and Ritchie R O 2017 On the question of
fractal packing structure in metallic glasses *Proc. Natl
Acad. Sci.* **114** 8458–63

[40] Wu Y, Wang H, Cheng Y, Liu X, Hui X, Nieh T, Wang Y and
Lu Z 2015 Inherent structure length in metallic glasses:
simplicity behind complexity *Sci. Rep.* **5** 12137

[41] Häussler P 1992 Interrelations between atomic and electronic
structures-liquid and amorphous metals as model systems
Phys. Rep. **222** 65–143

[42] Häussler P 1983 Evidence for a new Hume-Rothery phase
with an amorphous structure *Z. Phys.* B **53** 15–26

[43] Han G, Qiang J, Li F, Yuan L, Quan S, Wang Q, Wang Y,
Dong C and Häussler P 2011 The e/a values of ideal
metallic glasses in relation to cluster formulae *Acta Mater.*
59 5917–23

[44] Pang J, Tan M and Liew K 2013 On valence electron density,
energy dissipation and plasticity of bulk metallic glasses
J. Alloys Compd. **577** S56–S65

[45] Ashcroft N W and Mermin N D 1976 Solid state physics
(Philadelphia: Saunders College) Appendix N, 166 (2010)

[46] Bakonyi I, Ebert H and Liechtenstein A 1993 Electronic
structure and magnetic susceptibility of the different
structural modifications of Ti, Zr, and Hf metals *Phys. Rev.*
B **48** 7841–9

[47] Kanemaki S, Suzuki M, Yamada Y and Mizutani U 1988 Low
temperature specific heat, magnetic susceptibility and
electrical resistivity measurements in Ni-Ti metallic glasses
J. Phys. F **18** 105

[48] Yang W M *et al* 2014 Correlation of atomic packing
with the boson peak in amorphous alloys *J. Appl. Phys.*
116 123512

[49] Lewandowski J, Wang W and Greer A 2005 Intrinsic plasticity
or brittleness of metallic glasses *Phil. Mag. Lett.* **85** 77–87

[50] Li Y, Yu P and Bai H Y 2008 Study on the boson peak in bulk
metallic glasses *J. Appl. Phys.* **104** 013520

[51] Yang W, Liu H, Dun C, Li J, Zhao Y and Shen B 2013 Nearly
free electron model to glass-forming ability of
multi-component metallic glasses *J. Non-Cryst. Solids*
361 82–85

[52] Yu H B, Wang W H and Bai H Y 2010 An electronic structure
perspective on glass-forming ability in metallic glasses
Appl. Phys. Lett. **96** 081902

[53] Bai H Y, Luo J L, Zhang J and Chen Z J 2002 Low
temperature specific heat of a typical glass forming alloy
J. Appl. Phys. **91** 9123–7

[54] Kanemaki S, Takehira O, Fukamichi K and Mizutani U 1989
Low-temperature specific heats and magnetic properties of
$Co_{100-x}Zr_x$ metallic glasses over a wide concentration range
x= 10-80 *J. Phys.: Condens. Matter* **1** 5903

[55] Wang Z, Sun B and Lu J 2011 Effects of crystallization on
low-temperature specific heat capacity of $Cu_{60}Zr_{20}Hf_{10}Ti_{10}$
bulk metallic glass *Trans. Nonferr. Met. Soc. China*
21 1309–13

[56] Chen H and Haemmerle W 1972 Excess specific heat of a
glassy $Pd_{77.5}Cu_6Si_{16.5}$ alloy at low temperature
J. Non-Cryst. Solids **11** 161–9

[57] Li Y, Bai H, Wang W and Samwer K 2006 Low-temperature
specific-heat anomalies associated with the boson peak in
CuZr-based bulk metallic glasses *Phys. Rev.* B **74** 052201

[58] Hou L, Liu H, Liu Q, Dun C, Yang W, Huo J and
Dou L 2015 Effects of crystallization on boson peak of
$Zr_{52.5}Cu_{17.9}Ni_{14.6}Al_{10}Ti_5$ bulk metallic glass *J. Low Temp.
Phys.* **178** 11–17

[59] Yuan C C *et al* 2020 Impact of hybridization on metallic-glass
formation and design *Mater. Today* **32** 26–34

[60] Guan P F, Fujita T, Hirata A, Liu Y H and Chen M W 2012
Structural origins of the excellent glass forming ability of
$Pd_{40}Ni_{40}P_{20}$ *Phys. Rev. Lett.* **108** 175501

[61] Liu X F, Wang R J, Zhao D Q, Pan M X and Wang W H 2007
Bulk metallic glasses based on binary cerium and
lanthanum elements *Appl. Phys. Lett.* **91** 041901

[62] Steiner P, Hochst H and Hufner S 1977 XPS valence bands of
La, Ce and Gd and their aluminium alloys *J. Phys.* F
7 L145–9

[63] Kittel C 2005 *Introduction to Solid State Physics* (Beijing:
Chemical Industry Press)

[64] Luo Q and Wang W H 2009 Rare earth based bulk metallic
glasses *J. Non-Cryst. Solids* **355** 759–75

[65] Moruzzi V L, Oelhafen P, Williams A R, Lapka R,
Guntherodt H-J and Kubler J 1983 Theoretical and
experimental electronic structure of Zr-based
transition-metal glasses containing Fe, Co, Ni, Cu, Rh, and
Pd *Phys Rev.* B **27** 2049–54

[66] Garoche P and Bigot J 1983 Comparison between amorphous
and crystalline phases of copper-zirconium alloys by
specific-heat measurements *Phys. Rev.* B **28** 6886–95

[67] Vasiliev A N, Voloshok T N, Granato A V, Joncich D M,
Mitrofanov Y P and Khonik V A 2009 Relationship
between low-temperature boson heat capacity peak and
high-temperature shear modulus relaxation in a metallic
glass *Phys. Rev.* B **80** 172102

[68] Yang W M, Liu H S, Zhao Y C, Inoue A, Jiang K M, Huo J T,
Ling H B, Li Q and Shen B L 2014 Mechanical properties
and structural features of novel Fe-based bulk metallic
glasses with unprecedented plasticity *Sci. Rep.* **4** 6233

[69] Mizutani U, Takeuchi T and Sato H 2004 Interpretation of the
Hume-Rothery rule in complex electron compounds:
γ-phase Cu_5Zn_8 Alloy, FK-type $Al_{30}Mg_{40}Zn_{30}$ and MI-type
$Al_{68}Cu_7Ru_{17}Si_8$ 1/1–1/1–1/1 approximants *Prog. Mater.
Sci.* **49** 227–61

[70] Kumar G, Neibecker P, Liu Y H and Schroers J 2013 Critical
fictive temperature for plasticity in metallic glasses *Nat.
Commun.* **4** 1536